

Robust Diffusion Models for Adversarial Purification

Guang Lin^{1,2} Zerui Tao^{1,2} Jianhai Zhang³ Toshihisa Tanaka^{1,2} Qibin Zhao^{2,1}

Abstract

Diffusion models (DMs) based adversarial purification (AP) has shown to be the most powerful alternative to adversarial training (AT). However, these methods neglect the fact that pre-trained diffusion models themselves are not robust to adversarial attacks as well. Additionally, the diffusion process can easily destroy semantic information and generate a high quality image but totally different from the original input image after the reverse process, leading to degraded standard accuracy. To overcome these issues, a natural idea is to harness adversarial training strategy to re-train or fine-tune the pre-trained diffusion model, which is computationally prohibitive. We propose a novel robust reverse process with adversarial guidance, which is independent of given pre-trained DMs and avoids retraining or fine-tuning the DMs. This robust guidance can not only ensure to generate purified examples retaining more semantic content but also mitigate the accuracy-robustness trade-off of DMs for the first time, which also provides DM-based AP an efficient adaptive ability to new attacks. Extensive experiments are conducted to demonstrate that our method achieves the state-of-the-art results and exhibits generalization against different attacks.

1. Introduction

Deep neural networks (DNNs) have been shown to be vulnerable to adversarial examples (Szegedy et al., 2014), leading to disastrous implications. Since then, numerous methods have been proposed to defend against adversarial examples. Notably, adversarial training (AT, Goodfellow et al., 2015; Madry et al., 2018a) enhances classifiers by training with adversarial examples, achieving the state-of-the-art robustness against known attacks. However, when faced with

unseen attacks, AT is almost incapable of defense (Laidlaw et al., 2021; Dolatabadi et al., 2022). Another class of defense methods, adversarial purification (AP, Yoon et al., 2021), relies on pre-trained generative models to eliminate perturbations from potentially attacked images before classification. AP operates as a pre-processing step against unseen attacks without the need to retrain the classifier model. Recently, by leveraging the great generative capability of diffusion models (DMs, Ho et al., 2020; Song et al., 2020), Nie et al. (2022) achieved remarkable performance using AP and was shown to be a promising alternative to AT.

However, recent studies (Lee & Kim, 2023; Kang et al., 2023) find that DM-based AP is not as robust as shown in previous literature (Nie et al., 2022; Wang et al., 2022). Indeed, it might be easily fooled by attacks such as PGD+EOT. Moreover, by adding Gaussian noise, the perturbation is gradually destroyed, thereby enhancing the robust accuracy, but increasing Gaussian noise can also lead to a loss of semantic information, resulting in degraded accuracy. As a remedy, Wang et al. (2022); Anonymous (2023) propose the reverse processes with guidance to preserve semantic information. However, their guidance only considers suppressing example information loss, which lacks robustness against adversarial example information and has a risk of preserving or even enhancing adversarial perturbations. We argue that this is caused by the non-robustness of guidance, which is a crucial issue that needs to be solved. Therefore, our goal is to develop a diffusion model that can preserve semantic information while being robust to adversarial information.

To obtain a robust generator-based purifier, one possible solution is fine-tuning the generative model using adversarial examples and classification loss by freezing the classifier, which can thus preserve semantic information even under adversarial attacks. In particular, Lin et al. (2024) propose a defense pipeline called adversarial training on purification (AToP), which employs the adversarial loss to fine-tune the whole purifier and achieves great success in fine-tuning a robust AE-based purifier model (Wu et al., 2023) and GAN-based purifier model (Ughini et al., 2022). However, Lin et al. (2024) claim that AToP cannot work on DMs due to the high computational cost of generating adversarial examples for DMs. Therefore, the robustness of the DM-based purifier model still remains challenging.

In this paper, we propose a novel adversarial guided diffu-

¹Tokyo University of Agriculture and Technology ²RIKEN Center for Advanced Intelligence Project (RIKEN AIP) ³Hangzhou Dianzi University. Correspondence to: Qibin Zhao <qibin.zhao@riken.jp>.

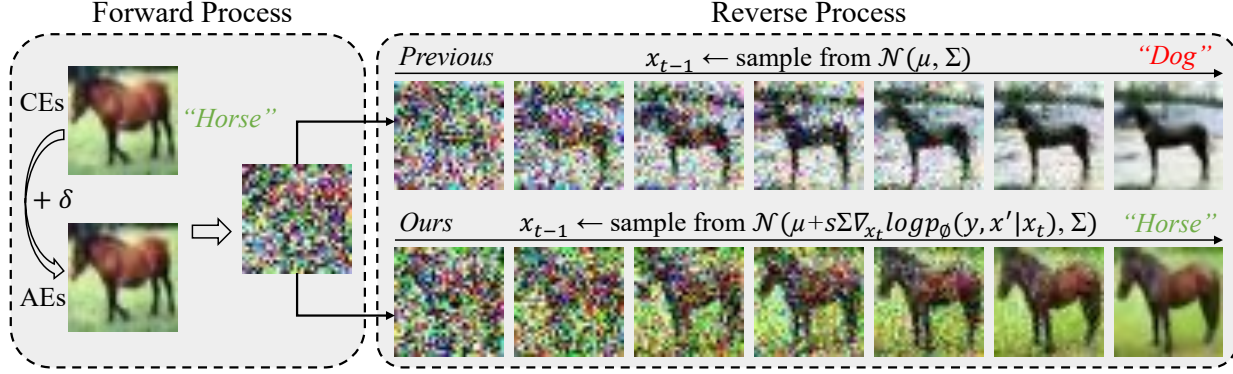


Figure 1. The scheme of diffusion-based purification. The clean examples (CEs) or adversarial examples (AEs) are firstly diffused with Gaussian noises by the forward process and then followed by the reverse process to remove the noise step by step. Unlike previous methods, our method can generate purified examples without changing its semantic information as well as classification label.

sion model (AGDM) that employs a robust reverse process with adversarial guidance of given pre-trained DMs, as illustrated in Figure 1. Notably, this robust guidance is independent of DMs and avoids retraining or fine-tuning the whole DMs. To achieve this, instead of training DMs, we train a robust guidance with a new adversarial loss and then apply this robust guidance to the reverse process of DMs during purification. Since our method does not need to compute the entire reverse process during training of robust guidance, it avoids the computational issue of ATOP. Given the robust guidance, the modified reverse process of DMs can not only generate better purified examples retaining more semantic content but also mitigate the accuracy-robustness trade-off. To the best of our knowledge, this is the first approach to consider accuracy-robustness trade-off in pre-trained generator-based AP, which might be a significant contribution to advance the development of this field.

To demonstrate the effectiveness of our method, we empirically evaluate the performance by comparing with the latest AT and AP methods across various attacks, including AutoAttack (Croce & Hein, 2020), StAdv (Xiao et al., 2018), PGD (Madry et al., 2018b) and EOT (Athalye et al., 2018), on CIFAR-10 and CIFAR-100 datasets under multiple classifier models. The experimental results demonstrate that our method achieves the state-of-the-art performance on both accuracy and robustness among AP baselines. Moreover, our method exhibits better robust generalization against unseen attacks. More importantly, our results on the robust evaluation of diffusion-based purification (Lee & Kim, 2023) manifest the necessity of robust guidance in diffusion models for adversarial purification.

Our contributions are summarized as follows.

- To enhance the robustness of diffusion models, we propose a robust reverse process to preserve semantic information and generate robust purified examples.

- An adversarial loss is proposed to train robust guidance, thus subtly bypassing the high computational demand when applying AT to DMs. It also provides a practical solution to mitigate the accuracy-robustness trade-off in DM-based AP.
- We conduct extensive experiments to empirically demonstrate that the proposed method significantly improves both the accuracy and robustness of diffusion-based purifier models, especially under the new robust evaluation scheme (Lee & Kim, 2023).

2. Preliminary

This section briefly review the adversarial training, adversarial purification, and diffusion models.

2.1. Adversarial Training and Adversarial Purification

Given a classifier c_γ with input x and output y , the adversarial attacks aim to find the adversarial examples x' that can fool the classifier model c_γ . The adversarial examples can be obtained by

$$x' = x + \delta, \quad \delta = \arg \max_{\delta \leq \varepsilon} \mathcal{L}(c_\gamma(x + \delta), y),$$

where δ represents a small perturbation and ε represents the maximum scale. To defend against adversarial attacks, the most popular technique is adversarial training (AT, Goodfellow et al., 2015; Madry et al., 2018a), which requires the classifier c_γ to be retrained with adversarial examples by

$$\min_{\gamma} \mathbb{E}_{p_{\text{data}}(x, y)} [\max_{\delta \leq \varepsilon} \mathcal{L}(c_\gamma(x + \delta), y)].$$

Another technique is adversarial purification (AP, Yang et al., 2019; Shi et al., 2021), which can purify the adversarial examples before feeding them into the classifier model, i.e.,

$$c_\gamma(g_\theta(x + \delta)) = c_\gamma(x),$$

where the purifier model g_θ in general does not require $g_\theta(x + \delta) = x$. As a plug-and-play module, the pre-trained generator-based purifier model can be integrated with any classifiers.

2.2. Diffusion Models

Diffusion models (Ho et al., 2020; Song et al., 2020) are a class of generative models that can generate high-quality images, which consist of two processes: a forward process transforms an image entirely into noise by gradually adding Gaussian noise, and a reverse process transforms noise into the generated image by gradually denoising.

In the denoising diffusion probabilistic model (DDPM, Ho et al., 2020), given a real image $x_0 \sim q(x)$, the forward process involves T steps, resulting in x_1, x_2, \dots, x_T . Since each step t is only related to the previous step $t-1$, it can also be viewed as a Markov process,

$$q(x_t | x_{t-1}) = \mathcal{N}(x_t; \sqrt{1 - \beta_t}x_{t-1}, \beta_t \mathbf{I}),$$

$$q(x_{1:T} | x_0) = \prod_{t=1}^T q(x_t | x_{t-1}),$$

where β_t , as a hyperparameter, is typically set to linearly interpolate from 0.0001 to 0.02 (Nichol et al., 2022). With $\alpha_t := 1 - \beta_t$ and $\bar{\alpha}_t := \prod_{s=1}^t \alpha_s$, any step t can be rewritten as one direct sample from

$$q(x_t | x_0) = \mathcal{N}(x_t; \sqrt{\bar{\alpha}_t}x_0, (1 - \bar{\alpha}_t)\mathbf{I}). \quad (1)$$

The reverse process aims to restore the original image x_0 from the Gaussian noise $x_T \sim \mathcal{N}(0, \mathbf{I})$ by sampling from $p_\theta(x_{t-1} | x_t)$, given by

$$p_\theta(x_{t-1} | x_t) = \mathcal{N}(x_{t-1}; \mu_\theta(x_t, t), \sigma_t^2 \mathbf{I}),$$

$$p_\theta(x_{0:T}) = p(x_T) \prod_{t=T}^1 p_\theta(x_{t-1} | x_t),$$

where σ_t denotes a time dependent constant and $\mu_\theta(x_t, t) = \frac{1}{\sqrt{\alpha_t}}x_t - \frac{1-\alpha_t}{\sqrt{1-\bar{\alpha}_t}\sqrt{\alpha_t}}\epsilon_\theta$ is usually modeled by a U-Net ϵ_θ , which needs to be trained to predict a random noise at each time step by Ho et al. (2020),

$$L(\theta) = \mathbb{E}_{t, x_0, \epsilon} [\|\epsilon - \epsilon_\theta(\sqrt{\bar{\alpha}_t}x_0 + \sqrt{1 - \bar{\alpha}_t}\epsilon, t)\|^2],$$

where $\epsilon \sim \mathcal{N}(0, \mathbf{I})$ denotes a Gaussian noise. Unlike the forward process, which can be directly computed by Eq. (1), the reverse process requires T steps to obtain x_0 from x_T . Therefore, as compared to other generative models, diffusion models are much slower in image generation.

3. Methods

We propose a novel adversarial guided diffusion model (AGDM) for adversarial purification, which purifies adversarial examples by a robust reverse process. We derive our

method in Section 3.1. Then, we discuss how to train a robust classifier and mitigate the accuracy-robustness trade-off in Section 3.2. Finally, we introduce the whole process of our diffusion-based purification in Section 3.3.

3.1. Adversarial Guided Diffusion Model

Unlike the guided diffusion (Dhariwal & Nichol, 2021; Wu et al., 2022; Kim et al., 2023; Anonymous, 2023), we are the first to introduce a robust classifier guidance to the reverse process. Similar to Dhariwal & Nichol (2021), we have

$$p_{\theta, \phi}(x_t | x_{t+1}, y, x') \propto p_\theta(x_t | x_{t+1})p_\phi(x' | x_t)p_\phi(y | x_t), \quad (2)$$

where x' is the adversarial example. To obtain this factorization of probabilities, we assume the label y and adversarial example x' are conditionally independent given x_t . The conditional distribution $p_\theta(x_t | x_{t+1})$ is characterized by the pre-trained diffusion model, while $p_\phi(x' | x_t)p_\phi(y | x_t)$ can be modeled by a robust classifier. In specific, $p_\phi(y | x_t)$ is the prediction of labels. Moreover, to describe relations between adversarial and diffused clean images, we adopt a heuristic probability,

$$p_\phi(x' | x_t) \propto \exp(-\mathcal{D}(f_\phi(x'), f_\phi(x_t))),$$

where $\mathcal{D}(\cdot, \cdot)$ is some distance measurement and f_ϕ is the classifier function that outputs the logit of labels.

For the first term in Eq. (2), we have

$$\log p_\theta(x_t | x_{t+1}) = -\frac{1}{2}(x_t - \mu)^\top \Sigma^{-1}(x_t - \mu) + C_1, \quad (3)$$

where μ and Σ are obtained by the pre-trained diffusion model and C_1 is a constant w.r.t. x_t . The second term in Eq. (2) can be approximated as

$$\begin{aligned} \log p_\phi(x' | x_t) &\approx \log p_\phi(x' | x_t) |_{x_t=\mu} + (x_t - \mu)^\top \nabla_{x_t} \log p_\phi(x' | x_t) |_{x_t=\mu} \\ &= (x_t - \mu)^\top \nabla_{x_t} \mathcal{D}(f_\phi(x'), f_\phi(x_t)) + C_2, \end{aligned} \quad (4)$$

where C_2 is a constant w.r.t. x_t . Finally, for the last term in Eq. (2), we have

$$\begin{aligned} \log p_\phi(y | x_t) &\approx \log p_\phi(y | x_t) |_{x_t=\mu} + (x_t - \mu)^\top \nabla_{x_t} \log p_\phi(y | x_t) |_{x_t=\mu} \\ &= (x_t - \mu)^\top g + C_3, \end{aligned} \quad (5)$$

where $g = \nabla_{x_t} \log p_\phi(y | x_t)$ and C_3 is a constant w.r.t. x_t . By plugging Eqs. (3) to (5) into Eq. (2), we obtain the adjusted score function with robust guidance,

$$\log p_{\theta, \phi}(x_t | x_{t+1}, y, x') = \log p(z) + C_4,$$

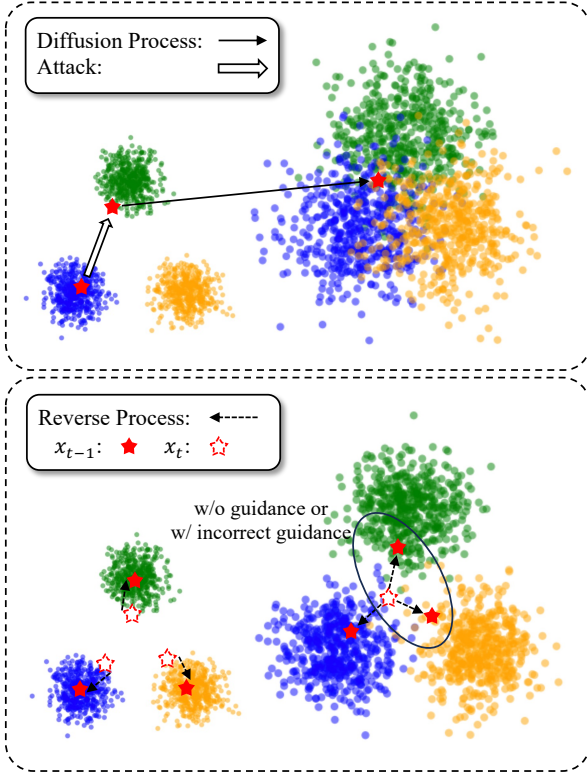


Figure 2. Overview of the diffusion process and reverse process. The movement of the red star represents the entire purification process. Different colored dots represent the data distributions of various categories. In the presence of attacks, without guidance or with incorrect guidance, the red star may move to the wrong category in the reverse process, thereby reducing robust accuracy.

where C_4 is a constant and z follows

$$z \sim \mathcal{N}(z; \mu + \Sigma g - \Sigma \nabla_{x_t} \mathcal{D}(f_\phi(x'), f_\phi(x_t)), \Sigma).$$

The full derivation is shown in Appendix A.1.

The above derivation of guided sampling is valid for DDPM. However, the robust reverse process can be extended to continuous-time diffusion models. Specifically, the denoising model ϵ_θ can be used to derive a score function (Song et al., 2020; Dhariwal & Nichol, 2021). Consider a diffusion process with drift coefficient $f(x, t)$ and diffusion coefficient $G(t)$, the robust reverse process becomes (details in Appendix A.2)

$$dx_t = [f(x, t) - G^2(t)(s_\theta + a_\phi + b_\phi)(x, t)] dt + G(t) d\bar{w},$$

where $s_\theta(x, t)$ is the pre-trained score network, $a_\phi(x, t) = \nabla_{x_t} \log p_\phi(y | x_t)$ and $b_\phi(x, t) = \nabla_{x_t} \log p_\phi(x' | x_t)$.

The proposed reverse process with robust guidance is presented in Algorithm 1. Note that a key challenge is to obtain the robust guidance for diffusion models. As we explained before, generating adversarial examples for the diffusion

Algorithm 1 Adversarial guided diffusion model, given a diffusion model $(\mu_\theta(x_t, t), \sigma_t)$, and scale s .

Input: Adversarial examples x'

Output: Purified examples x_0

$x_{t^*} \leftarrow$ sample from Eq. (7)

for t from t^* to 1 **do**

$\mu, \Sigma \leftarrow \mu_\theta(x_t, t), \sigma_t$

$x_{t-1} \leftarrow$ sample from $\mathcal{N}(\mu + s\Sigma \nabla_{x_t} \log p_\phi(y | x_t) - s\Sigma \nabla_{x_t} \mathcal{D}(f_\phi(x'), f_\phi(x_t)), \Sigma)$

end for

return x_0

model as in Lin et al. (2024) is infeasible. In the next subsection, we address this issue by a modification of the adversarial loss in Lin et al. (2024).

3.2. Robust Guidance Training

According to the above contents and adversarial training (Zhang et al., 2019), we train another robust classifier with classification loss on clean examples and discrepancy loss on adversarial examples and clean examples,

$$\min_{\phi} \mathbb{E}_{p_{\text{data}}(x, y)} [\underbrace{\mathcal{L}(f_\phi(x), y)}_{\text{for accuracy}} + \lambda \underbrace{\max_{\delta \leq \epsilon} \mathcal{D}(f_\phi(x), f_\phi(x'))}_{\text{for robustness}}], \quad (6)$$

where adversarial example $x' = x + \delta$, and λ is a weighting scale to balance the accuracy-robustness trade-off.

Unlike the previous work (Lin et al., 2024), they calculate the classification loss with adversarial examples $\mathcal{L}(f_\phi(x'), y)$ for fine-tuning to improve robust accuracy. Instead, we introduce discrepancy loss $\mathcal{D}(f_\phi(x), f_\phi(x'))$ to improve robustness while using only clean examples to calculate the classification loss $\mathcal{L}(f_\phi(x), y)$ to improve standard accuracy, details in Appendix B. To our best knowledge, this is the first to discuss the accuracy-robustness trade-off challenge in pre-trained generator-based purification.

3.3. Robust Reverse Process

The vanilla reverse process is vulnerable to adversarial attacks (Lee & Kim, 2023). During attacks, the vanilla classifier (Anonymous, 2023) may provide incorrect gradients, leading to incorrect guidance. Likewise, the reverse process without guidance can also lead to the sampling of noisy images towards incorrect labels, as shown in Figure 2. Considering this issue, we introduce additional adversarial information to sampling image from the robust reverse process.

Given an adversarial example x' , we first diffuse x' with t^* steps by

$$x_{t^*} = \sqrt{\bar{\alpha}_{t^*}} x' + \sqrt{1 - \bar{\alpha}_{t^*}} \epsilon, \quad \epsilon \sim \mathcal{N}(0, \mathbf{I}). \quad (7)$$

Then, in the robust reverse process, we can obtain the

purified example x_0 by sampling x_{t-1} from $\mathcal{N}(\mu + s\Sigma\nabla_{x_t} \log p_\phi(y, x' | x_t), \Sigma)$ with t^* steps. Note that we add scale s to adjust the guidance, which can be regarded as a temperature (Kingma & Dhariwal, 2018) in the distribution, i.e., $p_\phi(x' | x_t)^s p_\phi(y | x_t)^s$.

4. Related Work

Adversarial training (AT) is initially proposed by Goodfellow et al. (2015) to defend against adversarial attacks. While adversarial training has been demonstrated as an effective defense against attacks, it remains susceptible to unseen attacks (Stutz et al., 2020; Poursaeed et al., 2021; Laidlaw et al., 2021; Tack et al., 2022). Additionally, retraining the classifier model with only adversarial examples could severely impair the standard accuracy of the model (Kurakin et al., 2016; Madry et al., 2018b). To address this issue, Zhang et al. (2019); Pang et al. (2022) propose the loss functions that can effectively mitigate the trade-off between robustness and clean accuracy.

Adversarial purification (AP) purifies adversarial examples before classification, which has emerged as a promising defense method (Shi et al., 2021; Srinivasan et al., 2021). Compared with the AT method, AP utilizes a pre-trained generator that can defend against unseen attacks without retraining the classifier model (Song et al., 2018; Samangouei et al., 2018; Schott et al., 2019). For instance, Ughini et al. (2022) utilize a GAN-based generator and Nie et al. (2022) utilize a diffusion-based generator for adversarial purification. However, pre-trained generator-based AP methods cannot be adapted to known or new attacks, as the generator is trained without adversarial examples (Lee & Kim, 2023). To address this issue, Lin et al. (2024) propose adversarial training on purification (AToP), which fine-tunes the generator, enabling it to effectively defend against new attacks. However, the computational cost of AToP is highly related to the complexity of the generator model, rendering it impractical for application to diffusion models.

Diffusion model (DM) is a powerful generative model, achieving high-quality image generation (Ho et al., 2020; Song et al., 2020). Motivated by the great success of DMs, Yoon et al. (2021); Nie et al. (2022); Xiao et al. (2023); Carlini et al. (2023) utilize a pre-trained DM for adversarial purification and provided theoretical analysis, which acts as a solid foundation for diffusion-based purification. To better preserve semantic information, Wu et al. (2022); Wang et al. (2022) propose guided diffusion model for adversarial purification. Following a similar intention, Anonymous (2023) proposes a classifier-guided diffusion model to ensure the restoration of images with the target label.

However, all of the diffusion-based purification models do not consider the robustness of DMs, as shown in Lee & Kim

(2023); Kang et al. (2023) and our experiments. In the presence of attacks, the model can produce incorrect guidance, leading to a decrease in accuracy. Unlike previous works, we improve the inherent robustness of DMs by proposing a novel robust reverse process with adversarial guidance.

5. Experiments

In this section, we conduct extensive experiments on CIFAR-10 and CIFAR-100 across various classifier models on attack benchmarks. Compared with the state-of-the-art methods in Section 5.2, our method achieves optimal performance and exhibits generalization ability against unseen attacks. Furthermore, we undertake a more comprehensive evaluation scheme (Lee & Kim, 2023) in Section 5.3. Our method achieves the optimal average robust accuracy against PGD+EOT and AutoAttack.

5.1. Experimental Setup

Datasets and classifiers: We conduct extensive experiments on CIFAR-10 and CIFAR-100 (Krizhevsky et al., 2009) to empirically validate the effectiveness of the proposed methods against adversarial attacks. For the classifier models, we utilize the pre-trained ResNet (He et al., 2016) and WideResNet (Zagoruyko & Komodakis, 2016).

Adversarial attacks: We evaluate our method against AutoAttack l_∞ and l_2 threat models (Croce & Hein, 2020) as one benchmark, which is a powerful attack that combines both white-box and black-box attacks, and utilizes expectation over time (EOT, Athalye et al., 2018) to tackle the stochasticity introduced by random transforms. To consider unseen attacks without l_p -norm, we utilize spatially transformed adversarial examples (StAdv, Xiao et al., 2018) for evaluation. Additionally, following the guidance of Lee & Kim (2023), we utilize projected gradient descent (PGD, Madry et al., 2018b) with EOT for a more comprehensive evaluation of the diffusion-based purification.

Evaluation metrics: We evaluate the performance of defense methods using two metrics: standard accuracy and robust accuracy, obtained by testing on clean examples and adversarial examples, respectively. Due to the high computational cost of testing models with multiple attacks, following guidance by Nie et al. (2022), we randomly select 512 images from the test set for robust evaluation.

Training details: According to Zhang et al. (2019); Dhariwal & Nichol (2021) and experiments, we set the diffusion timestep $t^* = 70$, the scale $s = 1.0$, and the weighting scale $\lambda = 6.0$. Unless otherwise specified, all experiments presented in the paper are conducted under these hyperparameters and done using the NVIDIA RTX A5000 with 24GB GPU memory, CUDA v11.7 and cuDNN v8.5.0 in PyTorch v1.13.1 (Paszke et al., 2019).

Table 1. Standard accuracy and robust accuracy against AutoAttack l_∞ threat ($\epsilon = 8/255$) on CIFAR-10. ([†]the methods use additional synthetic images.)

Defense method	Extra data	Standard Acc.	Robust Acc.
Zhang et al. (2020)	✓	85.36	59.96
Gowal et al. (2020)	✓	89.48	62.70
Bai et al. (2023)	✓ [†]	95.23	68.06
Gowal et al. (2021)	× [†]	88.74	66.11
Wang et al. (2023)	× [†]	93.25	70.69
Peng et al. (2023)	× [†]	93.27	71.07
Rebuffi et al. (2021)	×	87.33	61.72
Nie et al. (2022)	×	89.02	70.64
Wang et al. (2022)	×	84.85	71.18
Anonymous (2023)	×	90.04	73.05
Ours	×	90.82	78.12

Table 2. Standard accuracy and robust accuracy against AutoAttack l_2 threat ($\epsilon = 0.5$) on CIFAR-10.

Defense method	Extra data	Standard Acc.	Robust Acc.
Augustin et al. (2020)	✓	92.23	77.93
Gowal et al. (2020)	✓	94.74	80.53
Wang et al. (2023)	× [†]	95.16	83.68
Ding et al. (2019)	×	88.02	67.77
Rebuffi et al. (2021)	×	91.79	78.32
Anonymous (2023)	×	92.58	83.13
Lee & Kim (2023)	×	90.16	86.48
Ours	×	90.82	86.84

5.2. Comparison with the state-of-the-art Methods

We evaluate our method on defending against AutoAttack l_∞ and l_2 threat models (Croce & Hein, 2020), and compare with the state-of-the-art methods on CIFAR-10 and CIFAR-100, as listed in RobustBench (Croce et al., 2021).

Result analysis on CIFAR-10: Table 1 shows the performance of the defense methods against AutoAttack l_∞ ($\epsilon = 8/255$) threat model on CIFAR-10 with WideResNet-28-10. In our method, the diffusion timestep is $t^* = 70$, with all other experimental settings remaining consistent. Our method outperforms all other methods without extra data (the dataset introduced by Carmon et al. (2019)) and additional synthetic data in terms of both standard accuracy and robust accuracy. Specifically, as compared to the second-best method, our method improves the robust accuracy by 5.07% and the standard accuracy by 0.78%.

Table 2 shows the performance of the defense methods against AutoAttack l_2 ($\epsilon = 0.5$) threat model on CIFAR-10 with WideResNet-28-10. Our method outperforms all methods in terms of robust accuracy. Specifically, as compared to the second-best method, our method improves the robust ac-

Table 3. Standard accuracy and robust accuracy against AutoAttack l_∞ threat ($\epsilon = 8/255$) on CIFAR-100.

Defense method	Extra data	Standard Acc.	Robust Acc.
Hendrycks et al. (2019)	✓	59.23	28.42
Cui et al. (2023)	× [†]	73.85	39.18
Wang et al. (2023)	× [†]	75.22	42.67
Pang et al. (2022)	×	63.66	31.08
Cui et al. (2023)	×	65.93	32.52
Ours	×	69.73	46.09

Table 4. Robust accuracy against AutoAttack l_∞ ($\epsilon = 8/255$) on CIFAR-10 and CIFAR-100, AutoAttack l_2 ($\epsilon = 0.5$) on CIFAR-10. (¹the method without guidance, ²the method with guidance, ³the method with robust guidance.)

Defense method	CIFAR 10, l_∞	CIFAR 10, l_2	CIFAR 100, l_∞
Nie et al. (2022) ¹	71.03	78.58	42.19
Anonymous (2023) ²	73.05	83.13	40.62
Ours ³	78.12	86.84	46.09

curacy by 0.36%. These results demonstrate that our method achieves the state-of-the-art performance in RobustBench (Croce et al., 2021).

Result analysis on CIFAR-100: Table 3 shows the performance of the defense methods against AutoAttack l_∞ ($\epsilon = 8/255$) threat model on CIFAR-100 with WideResNet-28-10. Our method outperforms all other methods without synthetic data in terms of both standard accuracy and robust accuracy. Specifically, as compared to the second-best method, our method improves the robust accuracy by 3.42%. The observations are basically consistent with CIFAR-10, further demonstrating the effectiveness of our method for adversarial purification.

Result analysis on guidance: Table 4 shows the robust accuracy of the three guidance patterns of diffusion model, i.e., the method without guidance (Nie et al., 2022), the method with guidance (Anonymous, 2023), and the method with robust guidance (ours). Our method achieves optimal robustness under all situations. Specifically, our method improves the robust accuracy by 5.07% against AutoAttack l_∞ , and by 3.71% against AutoAttack l_2 on CIFAR-10, respectively. Furthermore, it shows an improvement of 3.9% on CIFAR-100. The results demonstrate that our method can significantly improve the robustness of the pre-trained diffusion-based purifier model.

Result analysis on unseen attacks: As previously mentioned, unlike AT, AP can defend against unseen attacks, which is an important metric for evaluating AP. To demonstrate the generalization ability of AGDM, we conduct ex-

Table 5. Standard accuracy and robust accuracy against AutoAttack l_∞ ($\epsilon = 8/255$), l_2 ($\epsilon = 1$) and StAdv non- l_p ($\epsilon = 0.05$) threat models on CIFAR-10 with ResNet-50 model. We keep the same settings with Nie et al. (2022), where the diffusion timestep $t^* = 125$.

Defense method	Standard Acc.	AA l_∞	AA l_2	StAdv
Standard Training	94.8	0.0	0.0	0.0
Adv. Training with l_∞ (Laidlaw et al., 2021)	86.8	49.0	19.2	4.8
Adv. Training with l_2 (Laidlaw et al., 2021)	85.0	39.5	47.8	7.8
Adv. Training with StAdv (Laidlaw et al., 2021)	86.2	0.1	0.2	53.9
Adv. Training with all (Laidlaw et al., 2021)	84.0	25.7	30.5	40.0
PAT-self (Laidlaw et al., 2021)	82.4	30.2	34.9	46.4
Adv. CRAIG (Dolatatabadi et al., 2022)	83.2	40.0	33.9	49.6
DiffPure (Nie et al., 2022)	88.2	70.0	70.9	55.0
AGDM (Ours)	89.3	78.1	79.6	59.4

Table 6. Standard accuracy and robust accuracy against PGD+EOT (left: l_∞ , $\epsilon = 8/255$; right: l_2 , $\epsilon = 0.5$) on CIFAR-10 with WideResNet-28-10 model. We keep the same settings with Lee & Kim (2023), where the diffusion timestep $t^* = 100$. (¹the method without guidance, ²the method with guidance, ³the method with robust guidance.)

Type	Defense method	Extra data	Standard Acc.	Robust Acc.	Type	Defense method	Extra data	Standard Acc.	Robust Acc.
AT	Pang et al. (2022)	×	88.62	64.95	AT	Schwag et al. (2021)	×	90.93	83.75
	Gowal et al. (2020)	✓	88.54	65.93		Rebuffi et al. (2021)	✓	91.79	85.05
	Gowal et al. (2021)	×	87.51	66.01		Augustin et al. (2020)	×	93.96	86.14
AP	Yoon et al. (2021)	×	85.66	33.48	AP	Yoon et al. (2021)	×	85.66	73.32
	Nie et al. (2022) ¹	×	90.07	46.84		Nie et al. (2022) ¹	×	91.41	79.45
	Lee & Kim (2023)	×	90.16	55.82		Lee & Kim (2023)	×	90.16	83.59
	Wang et al. (2022) ²	×	93.50	24.06		Wang et al. (2022) ²	×	93.50	-
	Ours ³	×	90.42	64.06		Ours ³	×	90.42	85.55

periments under several different attacks with varying constraints (AutoAttack l_∞ , l_2 and StAdv non- l_p threat models) on CIFAR-10 with ResNet-50.

Table 5 shows that AT methods are limited in defending against unseen attacks and can only defend against known attacks (as indicated by the accuracy with an underscore) that they are trained with. In contrast, diffusion-based AP (DiffPure, Nie et al., 2022) demonstrates generalization capabilities to defend against all attacks. Our method further outperforms DiffPure in all situations. Specifically, it improves the robust accuracy by 8.1%, 8.7%, and 4.4% on AutoAttack l_∞ , l_2 and StAdv non- l_p , respectively. The results demonstrate that our method exhibits better generalization ability against unseen attacks.

5.3. Robust Evaluation of Diffusion-based Purification

AutoAttack is regarded as one of the strongest adversarial attacks and is acknowledged as a benchmark for evaluating various defense methods, as demonstrated in Section 5.2. However, Lee & Kim (2023) find that AutoAttack may not effectively evaluate the robustness of diffusion-based AP. Following the suggestions made by Croce et al. (2022), Lee & Kim (2023) provide a new pipeline (PGD+EOT) par-

ticularly for measuring the robustness of diffusion-based purification methods against adversarial attacks. To undertake a more comprehensive evaluation, we compare with the results in Lee & Kim (2023) in this subsection.

Result analysis on PGD+EOT: Table 6 shows the performance of the defense methods against PGD+EOT l_∞ ($\epsilon = 8/255$) and l_2 ($\epsilon = 0.5$) threat models on CIFAR-10 with WideResNet-28-10. Our method outperforms all AP methods in terms of robust accuracy. Specifically, as compared to the second-best method, our method improves the robust accuracy by 8.24% against l_∞ and by 1.96% against l_2 , respectively. Table 7 shows the results with WideResNet-70-16 and the observations are basically consistent with Table 6. These results demonstrate that our method achieves the state-of-the-art robustness in adversarial purification.

Result analysis on guidance: Furthermore, Table 6 also presents the results of three guidance patterns of diffusion model, i.e., the method without guidance (Nie et al., 2022), the method with guidance (Wang et al., 2022), and the method with robust guidance (ours). Due to the presence of guidance, the reverse process can generate better images without changing their semantic content, thereby improving classification accuracy. When without attacks, the method with guidance is highly effective, which has a 3.43% in-

Table 7. Standard accuracy and robust accuracy against PGD+EOT (left: l_∞ , $\epsilon = 8/255$; right: l_2 , $\epsilon = 0.5$) on CIFAR-10 with WideResNet-70-16. We keep the same settings with Lee & Kim (2023), where the diffusion timestep $t^* = 100$.

Type	Defense method	Extra data	Standard Acc.	Robust Acc.	Type	Defense method	Extra data	Standard Acc.	Robust Acc.
AT	Gowal et al. (2020)	✓	91.10	68.66	AT	Rebuffi et al. (2021)	×	92.41	86.24
	Gowal et al. (2021)	×	88.75	69.03		Gowal et al. (2020)	✓	94.74	88.18
	Rebuffi et al. (2021)	✓	92.22	69.97		Rebuffi et al. (2021)	✓	95.74	89.62
AP	Yoon et al. (2021)	×	86.76	37.11	AP	Yoon et al. (2021)	×	86.76	75.66
	Nie et al. (2022)	×	90.43	51.13		Nie et al. (2022)	×	92.15	82.97
	Lee & Kim (2023)	×	90.53	56.88		Lee & Kim (2023)	×	90.53	83.75
	Ours	×	90.43	66.41		Ours	×	90.43	85.94

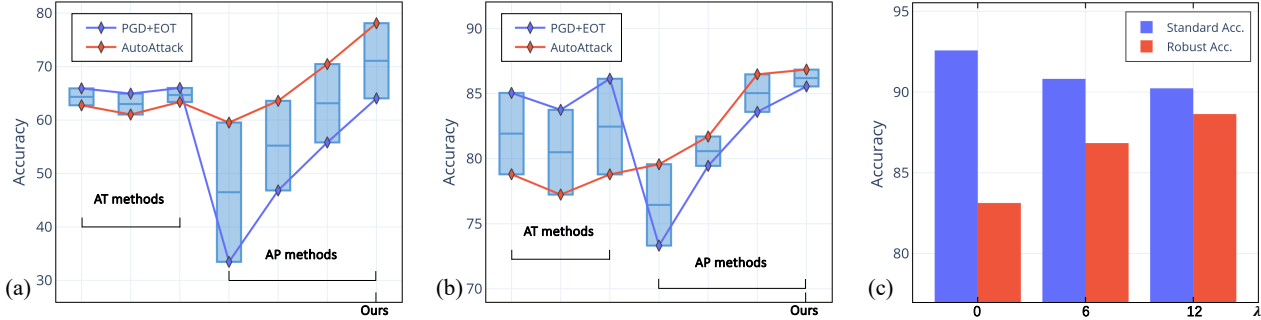


Figure 3. Comparison of robust accuracy against PGD+EOT and AutoAttack with (a) l_∞ ($\epsilon = 8/255$) threat model and (b) l_2 ($\epsilon = 0.5$) threat model on CIFAR-10 with WideResNet-28-10. The line in the middle of the box represents the average robust accuracy of two attacks. (c) Accuracy-robustness trade-off against AutoAttack l_2 ($\epsilon = 0.5$) threat model on CIFAR-10 with WideResNet-28-10.

crease in standard accuracy. However, they neglect the impact of attacks on guidance, leading to a 22.78% decrease in robust accuracy when facing attacks with full gradient. In contrast, our robust guided reverse process can achieve 17.22% increase in robust accuracy, which is significant.

Comparison between PGD+EOT and AutoAttack: Figure 3a and Figure 3b show the comparison between PGD+EOT and AutoAttack on l_∞ and l_2 threat models. Under different attacks, AT methods (Gowal et al., 2020; 2021; Pang et al., 2022) and AP methods (Yoon et al., 2021; Nie et al., 2022; Lee & Kim, 2023) exhibit significant differences in robust accuracy. AT performs better under PGD+EOT, while AP shows superior performance under AutoAttack. Typically, robustness evaluation is based on the worst-case results of the robust accuracy. Under this criterion, our method still outperforms all AT and AP methods. Furthermore, as compared to the second-best method on both attacks, our method improves the average robust accuracy by 6.39% against l_∞ and 1.16% against l_2 , respectively.

Accuracy-robustness trade-off: Figure 3c shows the performance against AutoAttack l_2 ($\epsilon = 0.5$) threat models on CIFAR-10 with different weighting scales λ . We observe that as the weighting scale λ increasing, the robust accuracy increases while the standard accuracy decreases, which ver-

ifies our Eq. (6) on the trade-off between robustness and accuracy.

6. Conclusion

In this paper, we propose an adversarial guided diffusion model (AGDM) for adversarial purification, which can enhance the robustness of diffusion models by a robust reverse process. Our innovative adversarial loss mechanism efficiently bypasses heavy computation of the entire reverse process in DMs during training and provides a practical solution to mitigate the accuracy-robustness trade-off. We conduct extensive experiments to empirically demonstrate that AGDM can significantly improve the robustness and generalization ability of diffusion-based purification.

Limitations: One limitation of diffusion-based adversarial purification is the time-consuming reverse process. In our experiments, evaluating the diffusion-based purifier against a single type of attack on 512 images requires ~ 13.8 hours on 4-A5000 node. Moreover, as compared to Nie et al. (2022), our method introduces additional hyperparameters s and λ , which need to be tuned in practice. We leave the study of utilizing our robust guidance in more advanced sampling strategies for future research.

Impact Statements

This paper presents work whose goal is to advance the field of Machine Learning. There are many potential societal consequences of our work, none of which we feel must be specifically highlighted here.

References

- Anderson, B. D. Reverse-time diffusion equation models. *Stochastic Processes and their Applications*, 12(3):313–326, 1982.
- Anonymous. Classifier guidance enhances diffusion-based adversarial purification by preserving predictive information, 2023. URL <https://openreview.net/forum?id=qvLPtx52ZR>.
- Athalye, A., Engstrom, L., Ilyas, A., and Kwok, K. Synthesizing robust adversarial examples. In *International conference on machine learning*, pp. 284–293. PMLR, 2018.
- Augustin, M., Meinke, A., and Hein, M. Adversarial robustness on in-and out-distribution improves explainability. In *European Conference on Computer Vision*, pp. 228–245. Springer, 2020.
- Bai, Y., Anderson, B. G., Kim, A., and Sojoudi, S. Improving the accuracy-robustness trade-off of classifiers via adaptive smoothing. *arXiv preprint arXiv:2301.12554*, 2023.
- Carlini, N., Tramer, F., Dvijotham, K. D., Rice, L., Sun, M., and Kolter, J. Z. (certified!!) adversarial robustness for free! In *The Eleventh International Conference on Learning Representations*, 2023.
- Carmon, Y., Raghuathan, A., Schmidt, L., Duchi, J. C., and Liang, P. S. Unlabeled data improves adversarial robustness. *Advances in neural information processing systems*, 32, 2019.
- Croce, F. and Hein, M. Reliable evaluation of adversarial robustness with an ensemble of diverse parameter-free attacks. In *International conference on machine learning*, pp. 2206–2216. PMLR, 2020.
- Croce, F., Andriushchenko, M., Sehwag, V., DeBenedetti, E., Flammarion, N., Chiang, M., Mittal, P., and Hein, M. Robustbench: a standardized adversarial robustness benchmark. In *Thirty-fifth Conference on Neural Information Processing Systems Datasets and Benchmarks Track (Round 2)*, 2021.
- Croce, F., Goyal, S., Brunner, T., Shelhamer, E., Hein, M., and Cemgil, T. Evaluating the adversarial robustness of adaptive test-time defenses. In *International Conference on Machine Learning*, pp. 4421–4435. PMLR, 2022.
- Cui, J., Tian, Z., Zhong, Z., Qi, X., Yu, B., and Zhang, H. Decoupled kullback-leibler divergence loss. *arXiv preprint arXiv:2305.13948*, 2023.
- Dhariwal, P. and Nichol, A. Diffusion models beat gans on image synthesis. *Advances in neural information processing systems*, 34:8780–8794, 2021.
- Ding, G. W., Sharma, Y., Lui, K. Y. C., and Huang, R. Mma training: Direct input space margin maximization through adversarial training. In *International Conference on Learning Representations*, 2019.
- Dolatabadi, H. M., Erfani, S., and Leckie, C. l-inf robustness and beyond: Unleashing efficient adversarial training. In *European Conference on Computer Vision*, pp. 467–483. Springer, 2022.
- Goodfellow, I. J., Shlens, J., and Szegedy, C. Explaining and harnessing adversarial examples. *International Conference on Learning Representations*, 2015.
- Goyal, S., Qin, C., Uesato, J., Mann, T., and Kohli, P. Uncovering the limits of adversarial training against norm-bounded adversarial examples. *arXiv preprint arXiv:2010.03593*, 2020.
- Goyal, S., Rebuffi, S.-A., Wiles, O., Stimberg, F., Calian, D. A., and Mann, T. A. Improving robustness using generated data. *Advances in Neural Information Processing Systems*, 34:4218–4233, 2021.
- He, K., Zhang, X., Ren, S., and Sun, J. Deep residual learning for image recognition. In *Proceedings of the IEEE conference on computer vision and pattern recognition*, pp. 770–778, 2016.
- Hendrycks, D., Lee, K., and Mazeika, M. Using pre-training can improve model robustness and uncertainty. In *International conference on machine learning*, pp. 2712–2721. PMLR, 2019.
- Ho, J., Jain, A., and Abbeel, P. Denoising diffusion probabilistic models. *Advances in neural information processing systems*, 33:6840–6851, 2020.
- Kang, M., Song, D., and Li, B. Diffattack: Evasion attacks against diffusion-based adversarial purification. In *Thirty-seventh Conference on Neural Information Processing Systems*, 2023.
- Kim, D., Kim, Y., Kwon, S. J., Kang, W., and Moon, I.-C. Refining generative process with discriminator guidance in score-based diffusion models. *International Conference on Machine Learning*, 2023.
- Kingma, D., Salimans, T., Poole, B., and Ho, J. Variational diffusion models. *Advances in neural information processing systems*, 34:21696–21707, 2021.

- Kingma, D. P. and Dhariwal, P. Glow: Generative flow with invertible 1x1 convolutions. *Advances in neural information processing systems*, 31, 2018.
- Krizhevsky, A., Hinton, G., et al. Learning multiple layers of features from tiny images. *Technical Report*, 2009.
- Kurakin, A., Goodfellow, I. J., and Bengio, S. Adversarial machine learning at scale. In *International Conference on Learning Representations*, 2016.
- Laidlaw, C., Singla, S., and Feizi, S. Perceptual adversarial robustness: Defense against unseen threat models. In *International Conference on Learning Representations (ICLR)*, 2021.
- Lee, M. and Kim, D. Robust evaluation of diffusion-based adversarial purification. In *Proceedings of the IEEE/CVF International Conference on Computer Vision (ICCV)*, pp. 134–144, October 2023.
- Lin, G., Li, C., Zhang, J., Tanaka, T., and Zhao, Q. Adversarial training on purification (atop): Advancing both robustness and generalization. *arXiv preprint arXiv:2401.16352*, 2024.
- Madry, A., Makelov, A., Schmidt, L., Tsipras, D., and Vladu, A. Towards deep learning models resistant to adversarial attacks. *International Conference on Learning Representations*, 2018a.
- Madry, A., Makelov, A., Schmidt, L., Tsipras, D., and Vladu, A. Towards deep learning models resistant to adversarial attacks. In *International Conference on Learning Representations*, 2018b.
- Nichol, A. Q., Dhariwal, P., Ramesh, A., Shyam, P., Mishkin, P., McGrew, B., Sutskever, I., and Chen, M. Glide: Towards photorealistic image generation and editing with text-guided diffusion models. In *International Conference on Machine Learning*, pp. 16784–16804. PMLR, 2022.
- Nie, W., Guo, B., Huang, Y., Xiao, C., Vahdat, A., and Anandkumar, A. Diffusion models for adversarial purification. *International Conference on Machine Learning*, 2022.
- Pang, T., Lin, M., Yang, X., Zhu, J., and Yan, S. Robustness and accuracy could be reconcilable by (proper) definition. In *International Conference on Machine Learning*, pp. 17258–17277. PMLR, 2022.
- Paszke, A., Gross, S., Massa, F., Lerer, A., Bradbury, J., Chanan, G., Killeen, T., Lin, Z., Gimelshein, N., Antiga, L., et al. Pytorch: An imperative style, high-performance deep learning library. *Advances in neural information processing systems*, 32, 2019.
- Peng, S., Xu, W., Cornelius, C., Hull, M., Li, K., Duggal, R., Phute, M., Martin, J., and Chau, D. H. Robust principles: Architectural design principles for adversarially robust cnns. *British Machine Vision Conference (BMVC)*, 2023.
- Poursaeed, O., Jiang, T., Yang, H., Belongie, S., and Lim, S.-N. Robustness and generalization via generative adversarial training. In *Proceedings of the IEEE/CVF International Conference on Computer Vision*, pp. 15711–15720, 2021.
- Rebuffi, S.-A., Goyal, S., Calian, D. A., Stimberg, F., Wiles, O., and Mann, T. Fixing data augmentation to improve adversarial robustness. *arXiv preprint arXiv:2103.01946*, 2021.
- Samangouei, P., Kabkab, M., and Chellappa, R. Defensegan: Protecting classifiers against adversarial attacks using generative models. *International Conference on Learning Representations*, 2018.
- Schott, L., Rauber, J., Bethge, M., and Brendel, W. Towards the first adversarially robust neural network model on mnist. *International Conference on Learning Representations*, 2019.
- Sehwag, V., Mahlouljifar, S., Handina, T., Dai, S., Xiang, C., Chiang, M., and Mittal, P. Robust learning meets generative models: Can proxy distributions improve adversarial robustness? In *International Conference on Learning Representations*, 2021.
- Shi, C., Holtz, C., and Mishne, G. Online adversarial purification based on self-supervision. *International Conference on Learning Representations*, 2021.
- Song, Y. and Ermon, S. Generative modeling by estimating gradients of the data distribution. *Advances in neural information processing systems*, 32, 2019.
- Song, Y., Kim, T., Nowozin, S., Ermon, S., and Kushman, N. Pixeldefend: Leveraging generative models to understand and defend against adversarial examples. *International Conference on Learning Representations*, 2018.
- Song, Y., Sohl-Dickstein, J., Kingma, D. P., Kumar, A., Ermon, S., and Poole, B. Score-based generative modeling through stochastic differential equations. In *International Conference on Learning Representations*, 2020.
- Srinivasan, V., Rohrer, C., Marban, A., Müller, K.-R., Samek, W., and Nakajima, S. Robustifying models against adversarial attacks by langevin dynamics. *Neural Networks*, 137:1–17, 2021.
- Stutz, D., Hein, M., and Schiele, B. Confidence-calibrated adversarial training: Generalizing to unseen attacks. In *International Conference on Machine Learning*, pp. 9155–9166. PMLR, 2020.

- Szegedy, C., Zaremba, W., Sutskever, I., Bruna, J., Erhan, D., Goodfellow, I., and Fergus, R. Intriguing properties of neural networks. *International Conference on Learning Representations*, 2014.
- Tack, J., Yu, S., Jeong, J., Kim, M., Hwang, S. J., and Shin, J. Consistency regularization for adversarial robustness. In *Proceedings of the AAAI Conference on Artificial Intelligence*, pp. 8414–8422, 2022.
- Ughini, G., Samele, S., and Matteucci, M. Trust-no-pixel: A remarkably simple defense against adversarial attacks based on massive inpainting. In *2022 International Joint Conference on Neural Networks (IJCNN)*, pp. 1–10. IEEE, 2022.
- Wang, J., Lyu, Z., Lin, D., Dai, B., and Fu, H. Guided diffusion model for adversarial purification. *arXiv preprint arXiv:2205.14969*, 2022.
- Wang, Z., Pang, T., Du, C., Lin, M., Liu, W., and Yan, S. Better diffusion models further improve adversarial training. *International conference on machine learning*, 2023.
- Wu, Q., Ye, H., and Gu, Y. Guided diffusion model for adversarial purification from random noise. *arXiv preprint arXiv:2206.10875*, 2022.
- Wu, Q., Ye, H., Gu, Y., Zhang, H., Wang, L., and He, D. Denoising masked autoencoders help robust classification. In *The Eleventh International Conference on Learning Representations*, 2023.
- Xiao, C., Zhu, J.-Y., Li, B., He, W., Liu, M., and Song, D. Spatially transformed adversarial examples. In *International Conference on Learning Representations*, 2018.
- Xiao, C., Chen, Z., Jin, K., Wang, J., Nie, W., Liu, M., Anandkumar, A., Li, B., and Song, D. Densepure: Understanding diffusion models for adversarial robustness. In *The Eleventh International Conference on Learning Representations*, 2023.
- Yang, Y., Zhang, G., Katabi, D., and Xu, Z. Me-net: Towards effective adversarial robustness with matrix estimation. *International Conference on Machine Learning*, 2019.
- Yoon, J., Hwang, S. J., and Lee, J. Adversarial purification with score-based generative models. In *International Conference on Machine Learning*, pp. 12062–12072. PMLR, 2021.
- Zagoruyko, S. and Komodakis, N. Wide residual networks. In *Proceedings of the British Machine Vision Conference 2016*. British Machine Vision Association, 2016.
- Zhang, H., Yu, Y., Jiao, J., Xing, E., El Ghaoui, L., and Jordan, M. Theoretically principled trade-off between robustness and accuracy. In *International conference on machine learning*, pp. 7472–7482. PMLR, 2019.
- Zhang, J., Zhu, J., Niu, G., Han, B., Sugiyama, M., and Kankanhalli, M. Geometry-aware instance-reweighted adversarial training. In *International Conference on Learning Representations*, 2020.

A. Proofs of Adversarial Guided Diffusion Model (AGDM)

A.1. Robust Reverse Process for DDPM

In the reverse process with adversarial guidance, similar to [Dhariwal & Nichol \(2021\)](#), we start by defining a conditional Markovian noising process \hat{q} similar to q , and assume that $\hat{q}(y, x' | x_0)$ is an available label distribution and adversarial example (AE) for each image.

$$\begin{aligned}\hat{q}(x_0) &:= q(x_0) \\ \hat{q}(y, x' | x_0) &:= \text{Label and AE per image} \\ \hat{q}(x_{t+1} | x_t, y, x') &:= q(x_{t+1} | x_t) \\ \hat{q}(x_{1:T} | x_0, y, x') &:= \prod_{t=1}^T \hat{q}(x_t | x_{t-1}, y, x').\end{aligned}\tag{8}$$

When \hat{q} is not conditioned on $\{y, x'\}$, \hat{q} behaves exactly like q ,

$$\begin{aligned}\hat{q}(x_{t+1} | x_t) &= \int_{y, x'} \hat{q}(x_{t+1}, y, x' | x_t) dy dx' \\ &= \int_{y, x'} \hat{q}(x_{t+1} | x_t, y, x') \hat{q}(y, x' | x_t) dy dx' \\ &= \int_{y, x'} q(x_{t+1} | x_t) \hat{q}(y, x' | x_t) dy dx' \\ &= q(x_{t+1} | x_t) \int_{y, x'} \hat{q}(y, x' | x_t) dy dx' \\ &= q(x_{t+1} | x_t) \\ &= \hat{q}(x_{t+1} | x_t, y, x').\end{aligned}\tag{9}$$

Following similar logic, we have: $\hat{q}(x_{1:T} | x_0) = q(x_{1:T} | x_0)$ and $\hat{q}(x_t) = q(x_t)$. From the above derivation, it is evident that the conditioned forward process is identical to unconditioned forward process. According to Bayes rule, the reverse process \hat{q} satisfies $\hat{q}(x_t | x_{t+1}) = q(x_t | x_{t+1})$.

$$\begin{aligned}\hat{q}(y, x' | x_t, x_{t+1}) &= \frac{\hat{q}(x_{t+1} | x_t, y, x') \hat{q}(y, x' | x_t)}{\hat{q}(x_{t+1} | x_t)} \\ &= \hat{q}(y, x' | x_t).\end{aligned}\tag{10}$$

For conditional reverse process $\hat{q}(x_t | x_{t+1}, y, x')$,

$$\begin{aligned}\hat{q}(x_t | x_{t+1}, y, x') &= \frac{\hat{q}(x_t, x_{t+1}, y, x')}{\hat{q}(x_{t+1}, y, x')} \\ &= \frac{\hat{q}(x_t, x_{t+1}, y, x')}{\hat{q}(y, x' | x_{t+1}) \hat{q}(x_{t+1})} \\ &= \frac{\hat{q}(x_t | x_{t+1}) \hat{q}(y, x' | x_t, x_{t+1}) \hat{q}(x_{t+1})}{\hat{q}(y, x' | x_{t+1}) \hat{q}(x_{t+1})} \\ &= \frac{\hat{q}(x_t | x_{t+1}) \hat{q}(y, x' | x_t, x_{t+1})}{\hat{q}(y, x' | x_{t+1})} \\ &= \frac{\hat{q}(x_t | x_{t+1}) \hat{q}(y, x' | x_t)}{\hat{q}(y, x' | x_{t+1})} \\ &= \frac{q(x_t | x_{t+1}) \hat{q}(y, x' | x_t)}{\hat{q}(y, x' | x_{t+1})}.\end{aligned}\tag{11}$$

Here $\hat{q}(y, x' | x_{t+1})$ does not depend on x_t . Then, by assuming the label y and adversarial example x' are conditionally independent given x_t , we can rewrite the above equation as $\hat{q}(x_t | x_{t+1}, y, x') = Z \cdot q(x_t | x_{t+1}) \hat{q}(x' | x_t) \hat{q}(y | x_t)$ where Z is a constant.

A.2. Robust Reverse Process for Continuous-time Diffusion Models

In the main text, we only showcased the preliminaries and the corresponding robust reverse process related to DDPM, but our method can also be extended to continuous-time diffusion models (Song et al., 2020). The continuous-time DMs build on the idea of DDPM, employ stochastic differential equations (SDE) to describe the diffusion process as follows,

$$dx = f(x, t)dt + G(t)dw, \quad (12)$$

where w represents a standard Brownian motion, $f(x, t)$ represents the drift of x_t and $G(t)$ represents the diffusion coefficient.

By starting from sample of Eq. 12 and reversing the process, Song et al. (2020) run backward in time and given by the reverse-time SDE,

$$dx = [f(x, t) - G(t)^2 \nabla_x \log p_t(x)]dt + G(t)d\bar{w}, \quad (13)$$

where \bar{w} represents a standard reverse-time Brownian motion and dt represents the infinitesimal time step. Similar to DDPM, the continuous-time diffusion model also requires training a network to estimate the time-dependent function $\nabla_x \log p_t(x)$. One common approach is to use a score-based model $s_\theta(x, t)$ (Song et al., 2020; Kingma et al., 2021). Subsequently, the reverse-time SDE can be solved by minimizing the score matching loss (Song & Ermon, 2019),

$$\mathcal{L}_\theta = \int_0^T \lambda(t) \mathbb{E}[\|s_\theta(x_t, t) - \nabla_{x_t} \log p_{0t}(x_t|x_0)\|^2] dt, \quad (14)$$

where $\lambda(t)$ is a weighting function, and p_{0t} is the transition probability from x_0 to x_t , where $x_0 \sim p_0(x)$ and $x_t \sim p_{0t}(x_t|x_0)$.

In the robust reverse process of continuous-time DMs, similar to Song et al. (2020), we suppose the initial state distribution is $p_0(x(0) | y, x')$ based on Eq. 13. Subsequently, using Anderson (1982) for the reverse process, we have

$$dx = \{f(x, t) - \nabla \cdot [G(t)G(t)^T] - G(t)G(t)^T \nabla_x \log p_t(x|y, x')\} dt + G(t)d\bar{w}. \quad (15)$$

Given a diffusion process x_t with SDE and score-based model $s_{\theta*}(x, t)$, we first observe that

$$\nabla_x \log p_t(x_t|y, x') = \nabla_x \log \int p_t(x_t|y_t, y, x') p(y_t|y, x') dy_t, \quad (16)$$

where y_t is defined via x_t and the forward process $p(y_t | x_t)$. Following the two assumptions by Song et al. (2020): $p(y_t | y, x')$ is tractable; $p_t(x_t|y_t, y, x') \approx p_t(x_t|y_t)$, we have

$$\begin{aligned} \nabla_x \log p_t(x_t|y, x') &\approx \nabla_x \log \int p_t(x_t|y_t) p(y_t|y, x') dy dx' \\ &\approx \nabla_x \log p_t(x_t|\hat{y}_t) \\ &= \nabla_x \log p_t(x_t) + \nabla_x \log p_t(\hat{y}_t|x_t) \\ &\approx s_{\theta*}(x_t, t) + \nabla_x \log p_t(\hat{y}_t|x_t), \end{aligned} \quad (17)$$

where \hat{y}_t is a sample from $p(y_t|y, x')$. Then, by assuming the label y and adversarial example x' are conditionally independent given x_t , we can update Eq. 13 with above formula, and obtain a new denoising model $\bar{\epsilon}$ with the guidance of label y and adversarial example x' ,

$$dx_t = [f(x, t) - G^2(t)(\nabla_x \log p_t(x) + \nabla_x \log p_t(y|x) + \nabla_x \log p_t(x'|x))(x, t)] dt + G(t) d\bar{w}. \quad (18)$$

B. Comparison with AGDM and AToP

To Enhance the existing pre-trained generator-based purification architecture to further improve robust accuracy against attacks. Lin et al. (2024) propose adversarial training on purification (AToP). Based on pre-trained model, they redesign the loss function to fine-tune the purifier model using adversarial loss.

Pre-training stage:

$$L_{\theta_g} = L_g(x, \theta_g). \quad (19)$$

Fine-tuning stage:

$$L_{\theta_g} = L_g(x', \theta_g) + s \cdot L_{cls}(x', y, \theta_g, \theta_f) = L_g(x', \theta_g) + s \cdot \max_{\delta} CE \{y, f(g(x', \theta_g))\}, \quad (20)$$

where L_g represents the original generative loss function of the generator model, which trained on clean examples and generates images similar to clean examples. During fine-tuning, AToP input the adversarial examples x' to optimize generator with generative loss, and further optimize the generator model with the adversarial loss L_{cls} , which is the cross-entropy loss between the output of x' and the ground truth y . However, training the generator with adversarial examples can lead to a decline in the performance on clean examples, thereby reducing standard accuracy. To address this issue, we modify back the input as x in two terms of L_{θ_g} and introduce a new constraint L_{dis} to enhance robust accuracy. To facilitate clearer comparison, we have used the same notation as AToP to represent our loss function, which differs from actual loss function.

$$\begin{aligned} L_{\theta_g} &= L_g(x, \theta_g) + s_1 \cdot L_{cls}(x, y, \theta_g, \theta_f) + s_2 \cdot L_{dis}(x, x', \theta_g, \theta_f) \\ &= L_g(x, \theta_g) + s_1 \cdot CE \{y, f(g(x, \theta_g))\} + s_2 \cdot KL \{f(g(x, \theta_g)), f(g(x', \theta_g))\}. \end{aligned} \quad (21)$$

Distinct from Eq. 20, in Eq. 21 we revert the input of the first two terms back to the clean examples x . By increasing the weight of s_1 , we can improve the standard accuracy on clean examples. Additionally, we introduce a new constraint term L_{dis} , which is the KL divergence between the feature map from the clean example x and the adversarial example x' . By increasing the weight of s_2 , we can improve the robust accuracy on adversarial examples. This effectively mitigates the accuracy-robustness trade-off issue.

C. Visualization

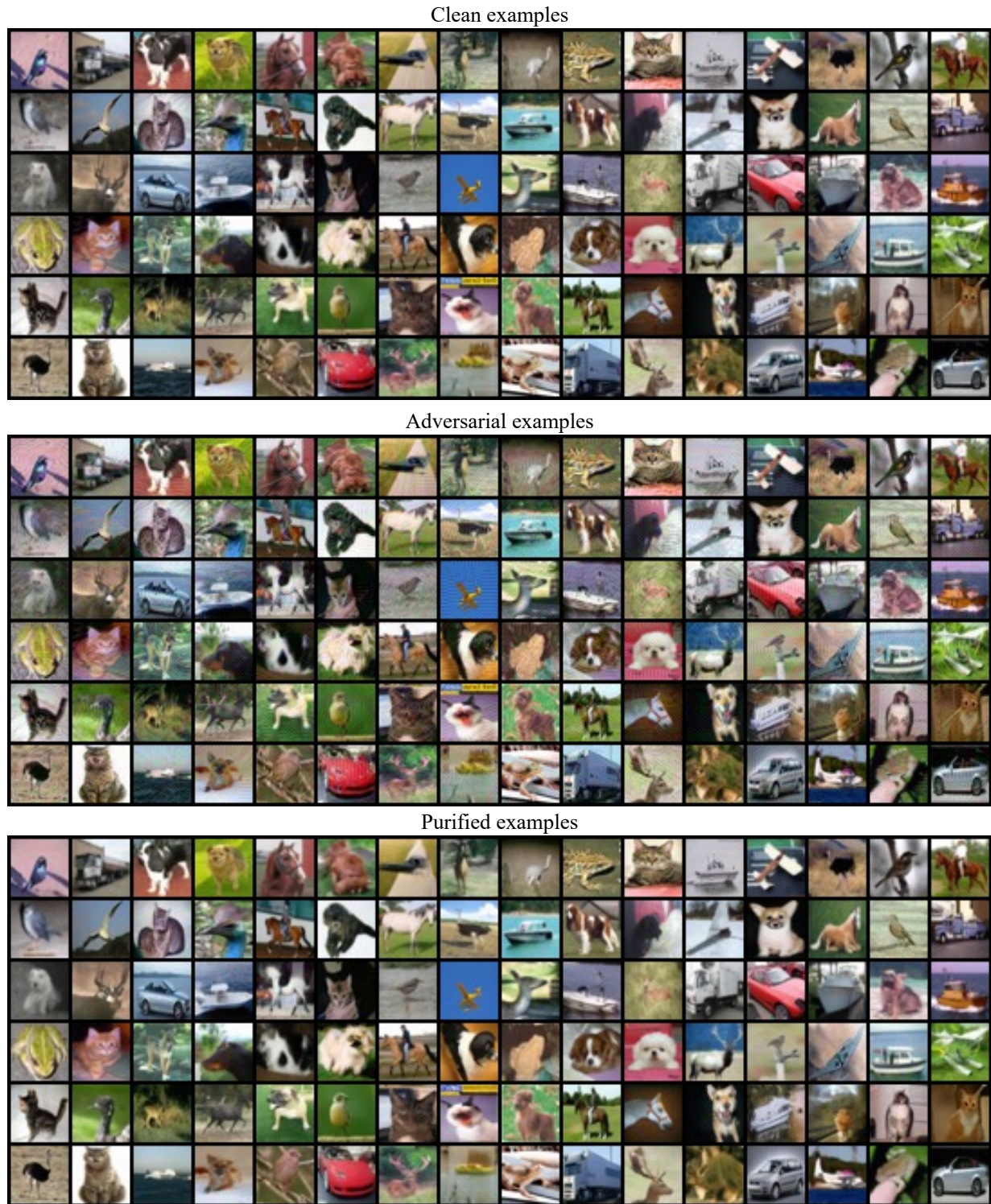


Figure 4. Clean examples (Top), adversarial examples (Middle) and purified examples (Bottom) of CIFAR-10.